https://doi.org/10.36375/prepare_u.iiche.a409

Photocatalytic Performance of Aluminum -Doped Graphene-like ZnO (g-AZO) Monolayer

S. Chowdhury[1], and Divya Somvanshi[2*]

[1]*Department of Electronics and Tele-Communication (ETCE) Engineering, Jadavpur University, Kolkata-700032, India*
[2]*Department of Physics, Harcourt Butler Technical University (HBTU), Kanpur-208002, India*
[*]*D. Somvanshi, Email: dsomvanshi@hbtu.ac.in, 8948930652*

Abstract

The graphene-like zinc oxide (g-ZnO) monolayer (ML) is a popular two-dimensional (2D) semiconductor. However, its applications are restricted in the photocatalytic water splitting reaction due to low visible absorption and wide optical band gap. Here, in this work, we studied the electronic structure of Al-doped graphene-like ZnO (g-AZO) ML using Density functional theory (DFT) calculations. The photocatalytic performance parameters such as bandgap, band edge levels, and absorption coefficient of g-AZO ML are studied under the application of biaxial strain varying from -10% to +10%. Our calculations show that g-AZO ML has a suitable band gap, band edge positions, and absorption coefficient in the visible range at ε = +9% and +10% tensile strain for photocatalytic water splitting reaction.

Keywords: Two-dimensional materials; Substitutional doping; biaxial strain; Photocatalysis reaction

I. Introduction

Photocatalytic water splitting is a promising technique for large-scale hydrogen production which uses renewable energy sources and also reduces global warming effects [1, 2]. For water splitting reaction, two conditions must be satisfied, first, the band edge positions must straddle the reduction and oxidation potentials of water.

Secondly, the band gap must exceed the hydrolysis voltage of water (1.23 eV) and be smaller than 3.00 eV [3, 4]. Recently, 2D semiconductors are being investigated for large-scale hydrogen production [4-9]. DFT tools allow the exploration of various external parameters to increase the photocatalytic performance of 2D materials [1, 10, 11]. The g-ZnO ML has high carrier mobility, large surface area, and excellent optical characteristics which enriches its applications in photocatalytic and energy harvesting fields [10-12]. Substitutional doping is considered one of the most desirable methods for tuning the electronic structure of semiconductors and it is also used to improve its photocatalytic performance [10, 11, 13-15]. Aluminium (Al) at the Zn site is considered an energetically favorable dopant in the g-ZnO ML. The g-AZO has various advantages such as reasonable cost, ample resources, tunable bandgap, and high stability in hydrogen plasma [16-22]. Although there are many studies have been reported on the improvement of the photocatalytic performance of 2D semiconductors by tuning the band gap [11, 23]. However, the photocatalytic properties of g-AZO ML have not been reported yet. Therefore, in this work, we investigated the photocatalytic properties of g-AZO ML under the application of biaxial strain using hybrid DFT calculations.

II. Computational details

Here, all the DFT calculations were performed using the Quantum ATK package [24]. The exchange-correlation functionals are described using hybrid functional (HSE06) [25]. A Linear combination of atomic orbitals (LCAO) basis with an energy cut-off of 125 Hartree and grid sampling of 25×25×1.

The dopant formation energy of Al in the g-ZnO monolayer is calculated as [26, 27], using

$$E_{form} = E_{ZnO+Al} - E_{ZnO} + \mu_{Zn} - \mu_{Al},$$

https://doi.org/10.36375/prepare_u.iiche.a409

The E_{form} of the g-AZO ML is calculated as -2.98 eV [28], which is exothermic in nature.

III. Results and discussions

A. Atomic and Electronic Structure of Al-doped ZnO monolayer

Here, we have doped one Al atom in a ZnO monolayer (4×4×1 supercell size) corresponding to a 6.25% doping concentration of the Al atom. The schematic atomic structure of g-AZO ML is shown in Fig. 1. The lattice constant and bond length for g-AZO ML is given as a = 3.29 Å, and d_{Al-O} = 1.77 Å [17]. The electronic band structure of g-AZO ML with HSE06 functionals has been shown in Fig. 2 and it is direct (Γ- Γ) in nature with a bandgap (E_g) value equal to 3.8 eV [17, 29].

It is observed that by doping an Al atom in the ZnO ML, the Fermi level shift inside the conduction band minima (CBM) resulted in n-type doping.

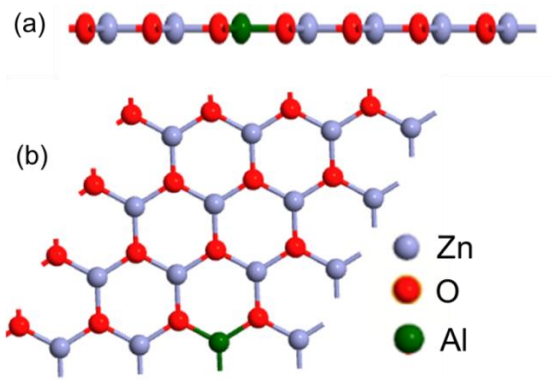

Fig. 1 (a) Side and (b) top view of the atomic structure of Al-doped g-ZnO monolayer,

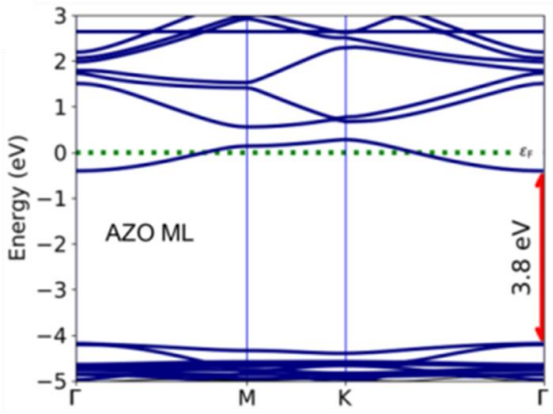

Fig. 2 Band structures of Al-doped ZnO ML obtained by HSE06 calculations.

B. Bandgap tunability of g-AZO monolayer under application of biaxial strain

Here, the effect of biaxial strain ($\varepsilon = \varepsilon_x = \varepsilon_y = (a_0 - a)/a \times 100\%$) on the electronic bandgap of the g-AZO ML is studied. The variations of bandgap under the application of varying biaxial strain from -10% to +10% are shown in Fig. 3. It is visible that the bandgap value linearly decreases with an increase in tensile strain from 0% to +9% and a slight increase at ε =+10% is observed. For compressive strain, the E_g value increases up to ε = -1% strain and then it starts decreasing continuously up to ε = -10%. We observed that the bandgap of g-AZO ML at +9% and +10% has decreased to 2.89 eV and 2.91 eV respectively, which satisfies the photocatalytic criteria for water splitting reaction [30].

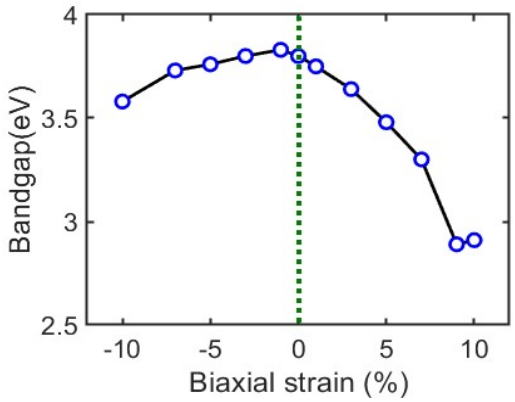

Fig. 3 Band gap of the g-AZO monolayer at different applied biaxial strains

C. Biaxial strain modulated optical spectra of g-AZO monolayer

The optical spectra of the g-AZO monolayer under varying biaxial strain are shown in Fig. 4. The absorption spectra at ε = 0% are shown by the black solid line. By increasing the tensile strain ε = 0% to +5%, a suppression of absorption spectra is observed in the UV and visible regions and it is shifted to red. However, a sharp peak is observed in the visible region at ε = +10% tensile strain (pink line). In the compressive strain up to ε = -5%, clampdown in UV and visible absorption have been observed with a blue shift. Interestingly, at ε = -10%, a sudden increase in absorption spectra occurs in the visible range.

https://doi.org/10.36375/prepare_u.iiche.a409

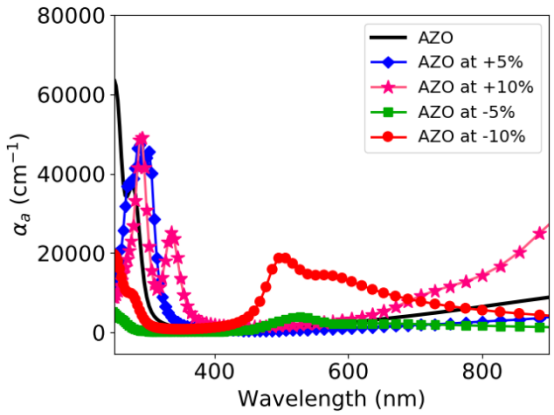

Fig. 4 Absorption spectra of the g-AZO monolayer with ε= ±5% and ±10%

D. Band edge positions of g-AZO monolayer under biaxial strain

Here, the band edge positions of g-AZO ML have been investigated by varying biaxial strain for analysis of photocatalytic performance. The band edge positions i. e. CBM, and VBM, under varying biaxial strain of the g-AZO monolayer, are shown in Fig. 5. It is noted that the g-AZO ML satisfies the band edge positions of CBM and VBM at unstrained conditions for water splitting. However, the bandgap energy of g-AZO ML at unstrained conditions exceeds bandgap of 3 eV which is not ideal for photocatalytic reaction. By applying biaxial tensile and compressive strain from -10% to +10%, the band edge positions of g-AZO ML have been tuned. The band edge positions of g-AZO ML initially reduces upto ε = +7% and then it started to increase. In the case of compressive strain, the band edge positions decrease continuously up to -9%. We found that the appropriate band edge positions for photocatalytic reaction have been observed at +9% and +10% tensile strain. At +9% and +10% tensile strain, the obtained CBM values are -4.41 eV, and -4.2 eV which are higher than H^+/H_2 (-4.44 eV) and the obtained VBM values are -7.3 eV, -7.11 eV which are lower than O_2/H_2O (-5.67 eV), respectively. The CBM level is located about 0.03 eV above the H^+/H^2 potential for +9% tensile strain. At +10% tensile strain, the CBM level increases to about 0.24 eV which is enough for hydrogen production. Meanwhile, the VBM level is always lower than the water oxidation potential (O_2/H_2O), and the oxidation capacity increases with the biaxial strain. The results show that the AZO ML has enough potential about 1.63 eV and 1.44 eV respectively for oxidation reaction at +9% and +10% tensile strain.

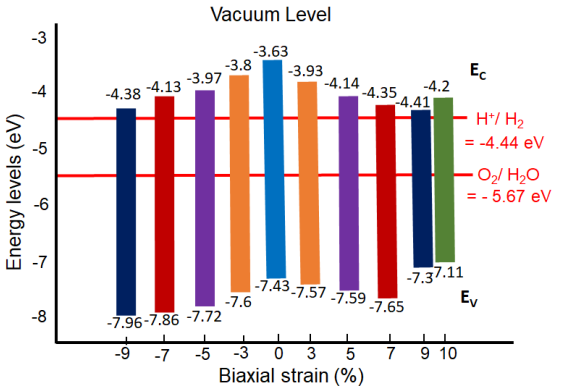

Fig. 5 CBM and VBM energy levels of g-AZO monolayer at unstrained and strained conditions.

Conclusion

In summary, the electronic structure and absorption spectra of g-AZO monolayer under varying biaxial strain have been studied by using hybrid DFT calculations for photocatalytic applications. Our results show that the g-AZO monolayer at ε = +9% and +10% has an appropriate bandgap, CBM, VBM positions for photocatalytic water splitting. Moreover, at ε = +10%, g-AZO ML shows good absorption in the visible region from 600 to 900 eV, which shows that biaxial strain can effectively modulate the photocatalytic performance of the g-AZO monolayer.

Acknowledgment

Divya Somvanshi thanks the DST INSPIRE Faculty Award (DST/INSPIRE/04/2017/000147) of the Government of India for the financial support.

References

[1] A. K. Singh, K. Mathew, H. L. Zhuang, and R. G. Hennig, "Computational Screening of 2D Materials for Photocatalysis," *The Journal of Physical Chemistry Letters*, vol. 6, pp. 1087-1098, 2015.

[2] P. Ganguly, M. Harb, Z. Cao, L. Cavallo, A. Breen, S. Dervin, *et al.*, "2D Nanomaterials for Photocatalytic Hydrogen Production," *ACS Energy Letters*, vol. 4, pp. 1687-1709, 2019.

https://doi.org/10.36375/prepare_u.iiche.a409

[3] S. Cho, J.-W. Jang, K.-H. Lee, and J. S. Lee, "Research Update: Strategies for efficient photoelectrochemical water splitting using metal oxide photoanodes," *APL Materials*, vol. 2, p. 010703, 2014.
[4] S. Hu and M. Zhu, "Ultrathin Two-Dimensional Semiconductors for Photocatalysis in Energy and Environment Applications," *ChemCatChem*, vol. 11, pp. 6147-6165, 2019.
[5] T. Hisatomi, J. Kubota, and K. Domen, "Recent advances in semiconductors for photocatalytic and photoelectrochemical water splitting," *Chemical Society Reviews*, vol. 43, pp. 7520-7535, 2014.
[6] Y. Ji, M. Yang, H. Dong, T. Hou, L. Wang, and Y. Li, "Two-dimensional germanium monochalcogenide photocatalyst for water splitting under ultraviolet, visible to near-infrared light," *Nanoscale*, vol. 9, pp. 8608-8615, 2017.
[7] B. Luo, G. Liu, and L. Wang, "Recent advances in 2D materials for photocatalysis," *Nanoscale*, vol. 8, pp. 6904-6920, 2016.
[8] Y. Li, Y.-L. Li, B. Sa, and R. Ahuja, "Review of two-dimensional materials for photocatalytic water splitting from a theoretical perspective," *Catalysis Science & Technology*, vol. 7, pp. 545-559, 2017.
[9] S. J. A. Moniz, S. A. Shevlin, D. J. Martin, Z.-X. Guo, and J. Tang, "Visible-light driven heterojunction photocatalysts for water splitting – a critical review," *Energy & Environmental Science*, vol. 8, pp. 731-759, 2015.
[10] H. Chen, C. Tan, K. Zhang, W. Zhao, X. Tian, and Y. Huang, "Enhanced photocatalytic performance of ZnO monolayer for water splitting via biaxial strain and external electric field," *Applied Surface Science*, vol. 481, pp. 1064-1071, 2019.
[11] T. Kaewmaraya, A. De Sarkar, B. Sa, Z. Sun, and R. Ahuja, "Strain-induced tunability of optical and photocatalytic properties of ZnO mono-layer nanosheet," *Computational Materials Science*, vol. 91, pp. 38-42, 2014.
[12] K. K. Korir, E. M. Benecha, F. O. Nyamwala, and E. B. Lombardi, "Tuning electronic structure of ZnO nanowires via 3d transition metal dopants for improved photo-electrochemical water splitting: An ab initio study," *Materials Today Communications*, vol. 26, p. 101929, 2021.
[13] I. Ahmad, E. Ahmed, and M. Ahmad, "The excellent photocatalytic performances of silver doped ZnO nanoparticles for hydrogen evolution," *SN Applied Sciences*, vol. 1, p. 327, 2019.
[14] D. Commandeur, J. McGuckin, and Q. Chen, "Hematite coated, conductive Y doped ZnO nanorods for high-efficiency solar water splitting," *Nanotechnology*, vol. 31, p. 265403, 2020.
[15] R. Dom, L. R. Baby, H. G. Kim, and P. H. Borse, "Enhanced Solar Photoelectrochemical Conversion Efficiency of ZnO:Cu Electrodes for Water-Splitting Application," *International Journal of Photoenergy*, vol. 2013, p. 928321, 2013.
[16] C.-H. Zhai, R.-J. Zhang, X. Chen, Y.-X. Zheng, S.-Y. Wang, J. Liu, *et al.*, "Effects of Al Doping on the Properties of ZnO Thin Films Deposited by Atomic Layer Deposition," *Nanoscale Research Letters*, vol. 11, p. 407, 2016.
[17] Q. Fan, J. H. Yang, Y. Yu, J. P. Zhang, and J. Cao, "Electronic Structure and Optical Properties of Al-doped ZnO from Hybrid Functional Calculations," *Chemical Engineering Transactions*, vol. 46, pp. 985-990, 2015.
[18] R. Mahdavi and S. S. A. Talesh, "Sol-gel synthesis, structural and enhanced photocatalytic performance of Al-doped ZnO nanoparticles," *Advanced Powder Technology*, vol. 28, pp. 1418-1425, 2017.
[19] F. Maldonado and A. Stashans, "Al-doped ZnO: Electronic, electrical and structural properties," *Journal of Physics and Chemistry of Solids*, vol. 71, pp. 784-787, 2010.
[20] R. Saniz, Y. Xu, M. Matsubara, M. N. Amini, H. Dixit, D. Lamoen, *et al.*, "A simplified approach to the band gap correction of defect formation energies: Al, Ga, and In-doped ZnO," *Journal of Physics and Chemistry of Solids*, vol. 74, pp. 45-50, 2013.
[21] Y.-F. Xu, H.-S. Rao, X.-D. Wang, H.-Y. Chen, D.-B. Kuang, and C.-Y. Su, "In situ formation of zinc ferrite modified Al-doped ZnO nanowire arrays for solar water splitting," *Journal of Materials Chemistry A*, vol. 4, pp. 5124-5129, 2016.
[22] X. Zhang, Y. Chen, S. Zhang, and C. Qiu, "High photocatalytic performance of high concentration Al-doped ZnO nanoparticles," *Separation and Purification Technology*, vol. 172, pp. 236-241, 2017.
[23] B. Sa, Y.-L. Li, J. Qi, R. Ahuja, and Z. Sun, "Strain Engineering for Phosphorene: The Potential Application as a Photocatalyst," *The Journal of Physical Chemistry C*, vol. 118, pp. 26560-26568, 2014.
[24] S. Smidstrup, T. Markussen, P. Vancraeyveld, J. Wellendorff, J. Schneider, T. Gunst, *et al.*, "QuantumATK: an integrated platform of electronic and atomic-scale modeling tools," *J. Condens. Matter Phys.*, vol. 32, p. 015901, 2019.
[25] J. Carmona-Espíndola, J. L. Gázquez, A. Vela, and S. B. Trickey, "Generalized Gradient Approximation Exchange Energy Functional with Near-Best Semilocal Performance," *J. Chem. Theory Comput.*, vol. 15, pp. 303-310, 2019.
[26] X. Zhao, P. Chen, and T. Wang, "Controlled electronic and magnetic properties of WSe2 monolayers by doping transition-metal atoms," *Superlattices and Microstructures*, vol. 100, pp. 252-257, 2016.
[27] S. Liu, S. Huang, H. Li, Q. Zhang, C. Li, X. Liu, *et al.*, "Tunable electronic behavior in 3d transition metal doped 2H-WSe2," *Physica E: Low-dimensional Systems and Nanostructures*, vol. 87, pp. 295-300, 2017.
[28] S. Chowdhury, P. Venkateswaran, and D. Somvanshi, "A systematic study on the electronic structure of 3d, 4d, and 5d transition metal-doped WSe2 monolayer," *Superlattices and Microstructures*, vol. 148, p. 106746, 2020.
[29] D. Sun, C. Tan, X. Tian, and Y. Huang. (2017, 2017/06//). Comparative Study on ZnO Monolayer Doped with Al, Ga and In Atoms as Transparent Electrodes. *Materials (Basel, Switzerland) 10(7)*. Available:
[30] S. Chowdhury, P. Venkateswaran, and D. Somvanshi, "Strain-dependent doping and optical absorption in Al-doped graphene-like ZnO monolayer," *Solid State Communications*, vol. 365, p. 115139, 2023.